Elevated Temperature Mechanical Properties of Al-Li-Cu-Mg Alloy

When compared to Alloy 2024, Al-Li Alloy 2091 displays favorable strength, superior ductility and less susceptibility to HAZ cracking

BY T. ZACHARIA AND D. K. AIDUN

ABSTRACT. A detailed experimental investigation was carried out to characterize the elevated temperature mechanical properties of aluminum-lithium Alloy 2091. Gleeble hot tensile tests were conducted to evaluate the relative elevated temperature strength and ductility of Al-Li-Cu-Mg (2091) and Al-Cu-Mg (2024) alloys. In general, Alloy 2091 in the "as-cast" condition exhibited very low elevated temperature strength and ductility for all the test conditions. This was attributed to the coarse dendritic structure of the as-cast material. The hot tensile tests indicated that the tensile strength of the wrought Alloy 2091 adequately matched the strength of Alloy 2024 throughout the temperature regime.

The weld heat-affected zone (HAZ) hot-cracking susceptibility of the two aluminum alloys was also evaluated using the Gleeble thermal-mechanical simulator. The results of hot ductility tests show that Alloy 2091 in the wrought form exhibits superior ductility throughout the range of temperatures investigated. Based on the recovery of ductility from the nil ductility temperature (NDT), Alloy 2091 was judged to be crack resistant in the weld metal HAZ.

Introduction

In recent years, there has been considerable interest devoted to aluminum-lithium alloys due to their reduced density and increased elastic modulus compared with conventional aluminum alloys. Addition of lithium, as an alloying element, decreases the density and increases the elastic modulus of aluminum alloys (Refs. 1–3). Given the potential of this lightweight, high-stiffness material for aerospace application, a number of primary producers of aluminum and other research organizations have stepped up their research activities in developing a new generation of aluminum-lithium alloys. Al-Li-Cu-Mg Alloy 2091 is one of the new-generation aluminum-lithium alloys intended to have combinations of strength, toughness and damage-tolerant properties comparable with those of Alloy 2024 (Ref. 4).

The purpose of determining the elevated temperature mechanical properties of any material is to determine its endurance limits in a number of practical applications to which it may be subjected, at temperatures approaching and exceeding the melting point. Among such operations are welding and casting, which involve fusion of the metal. In any weldment, low-melting minor elements, impurities or eutectic phases can ultimately cause hot-cracking. This is also true for aluminum-lithium alloys. Cracking that is normally intergranular can occur in both the weld metal and the associated heat-affected zone, especially under conditions of high restraint. Heat-affected-zone cracking in a range of alloys has been associated with low ductility during cooling from peak temperatures at and above the melting point of the alloy. For proper design of a joining process (welding), reliable measurements of the elevated temperature mechanical behavior and hot-cracking susceptibility of the alloy being used are essential.

A number of investigators (Refs. 5–7) have successfully determined the elevated temperature mechanical properties of aluminum alloys with the object of relating these properties with crack susceptibility. The impact resistance at elevated temperatures of several commercial aluminum alloys was evaluated by Archbutt, *et al.* (Ref. 5), and found that the resistance to shock was very low at the point of incipient fusion. It was postulated that the alloys exhibiting rapid recovery of impact resistance, with fall in temperature immediately below the solidus, would exhibit a lower susceptibility to cracking than alloys in which the recovery was more gradual.

Singer and Cottrell (Ref. 6) determined the elevated temperature tensile properties of ten Al-Si alloys at temperatures both above and below the equilbrium solidus. The alloys were heated to a preselected temperature and held at that temperature for sufficient time for attaining structural equilibrium. The specimens were then tested at temperature, at a constant strain rate. Their results show that all the alloys exhibit a sudden loss in strength and complete loss of ductility at the point of incipient fusion. Above this temperature, the alloys failed with brittle, intercrystalline fractures. The extent of this temperature range was found to be a function of the composition of the alloy. Pumphrey and Jennings (Ref. 7) determined the high-temperature tensile properties of Al-Si alloys during cooling from the liquid state and during rapid heating from room temperature. Their results show that the material exhibits lower strength on cooling from the solidus.

Evaluation of hot ductility is another method of determining the heat-affected zone hot-cracking susceptibility of many alloys. The test is based on the premise that the deformation behavior of a material during a given thermal cycle should reflect its cracking tendency. In principle,

KEY WORDS

Al-Li-Cu-Mg Alloy
As-Cast 2091 Alloy
Wrought Alloy 2091
Mechanical Properties
Elevated Temperature
Binary Al-Li Alloy
Hot Cracking
Nil Strength
Hot Ductility Tests
Crack Sensitivity

T. ZACHARIA is with the Metals and Ceramics Division, Oak Ridge National Laboratory, Oak Ridge, Tenn. D. K. AIDUN is with the Department of Mechanical Engineering, Clarkson University, Potsdam, N.Y.

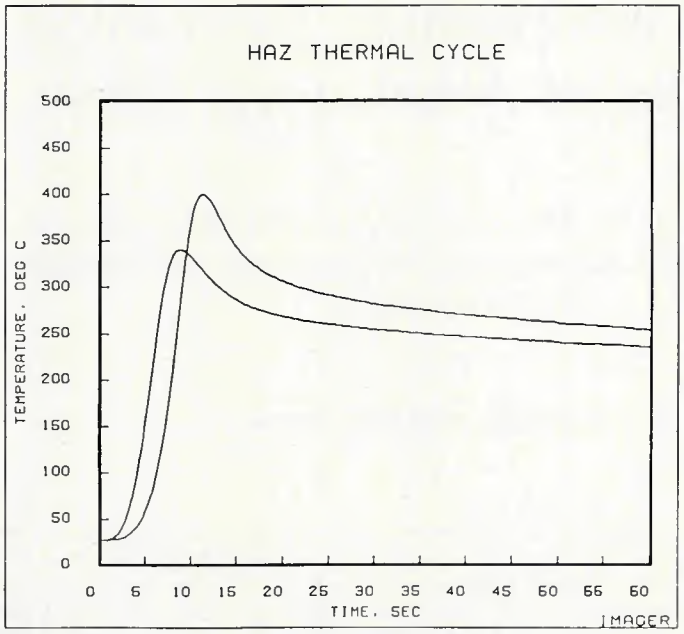

Fig 1 — Weld metal HAZ thermal cycle

a hot ductility test involves making hot tensile tests at preselected temperatures during heating and cooling in an attempt to reproduce the strength and ductility of the material during welding. The segregation present in the microstructure would allow the formation of low-melting constituents that often wet grain boundaries and cause a loss of both mechanical strength and ductility. The greater the temperature range over which this liquation phenomenon occurs, the greater the susceptibility to hot cracking.

Nippes, *et al.* (Ref. 8), developed the technique of using the Gleeble thermal mechanical simulator to evaluate HAZ crack susceptibility. The thermal mechanical simulator allows the modeling of rapid thermal cycles found in the heat-affected zone during fusion welding. Both flat and cylindrical specimens have been used in various studies of weldability and hot ductility (Refs. 9, 10). Recently, Balaguer, *et al.* (Ref. 11), examined the hot ductility behavior of Al-4Mg-2Li and Al-3.5Mg-4Zn alloys to evaluate their relative crack susceptibilities. Their tests show that the lithium-containing alloy has a relatively lower ductility and, therefore, higher crack susceptibility.

Experimental Procedure

The materials used in this investigation comprise two heats of Alloy 2091, one each, in the as-cast and in the T3 condition and one heat of Alloy 2024 in the T3 condition. Compositions of these alloys are given in Table 1. Cylindrical specimens of 6-mm (0.24-in.) diameter were machined from all three heats for the Gleeble tests. For test temperatures below 350°C (660°F), specimens from each heat were machined with a reduced center section to ensure that fracture took place within the gauge length.

Elevated temperature tests were performed using a Duffers Scientific, Gleeble Model 1500. The Gleeble is a programmed thermal-mechanical testing machine that can be used to simulate the thermal cycle associated with the GTAW process. The accuracy of the thermal servo is ±1°C (1.8°F) at equilibrium and ±2°C (3.6°F) at 150°C/s (300°F/s) rate, per the manufacturer's specifications. It can also be used to strain specimens in either tension or compression while being heated by resistance heating. A two-wire chromel-alumel thermocouple was percussion welded to the specimen to provide required temperature control. Elevated temperature tensile tests with a stroke rate of 0.635 mm/s (0.025 in./s) were performed on cylindrical specimens for both heating and cooling conditions. Tests at preselected temperatures were performed immediately upon reaching the temperature.

The determination of the HAZ mechanical properties involved producing a microstructure, in the Gleeble specimen, typical of a portion of the HAZ of the weldment. Autogenous bead-on-plate welds were made on 250- × 64- × 12-mm (10- × 2.5- × 0.5-in.) specimens in a He atmosphere. Welding was carried out by a Hobart, Cyber Tig 100 series, welding machine at 170 A, 14 V and 3.4 mm/s (8 ipm), using 3.18-mm 2% thoriated tungsten electrode. The weld HAZ thermal cycles were obtained using a Digital Equipment Corporation, MINC (modular instrument computer) and chromel-alumel thermocouple. Two thermocouples were located in the HAZ, 10 mm and 9 mm from the weld centerline on the top surface of the specimen. The resulting thermal cycle is shown in Fig. 1.

Table 1—Alloy Composition (wt-%)

Element	2091-AC	2091-T3	2024-T3
Si	0.04	0.03	0.09
Fe	0.05	0.05	0.30
Cu	2.00	1.80	4.00
Mn	0.00	0.00	0.60
Mg	1.30	1.40	1.40
Cr	0.00	0.00	0.00
Zn	0.02	0.01	0.09
Li	2.30	1.70	0.00
Zr	0.09	0.09	0.00
Ti	0.01	0.01	0.03

Microstructural characterization was done by optical and scanning electron microscopy. Longitudinal sections from all three heats were prepared from the specimens near the fractured tip for metallographic inspection. All metallographic specimens were prepared using standard procedures and then etched using Keller's reagent.

Results and Discussion

Fusion joining by a conventional welding process is a key issue in the development and commercial exploitation of aluminum-lithium alloys. During welding, the weld metal and the adjacent heat-affected zone are subjected to extremely high temperatures. Figure 2 shows the numerically computed temperature distribution in the longitudinal and transverse section of a typical GTA weld made on an aluminum alloy (Ref. 12). The calculated temperature gradients near the weld are of the order of 2800°C/cm (12,283°F/in.). The relatively large temperature gradients can generate thermal stresses and strains that can ultimately cause hot-cracking in the fusion zone and the heat-affected zone. Therefore, it is important to characterize the elevated temperature behavior of the material under conditions that are similar to those that occur during welding. The present investigation focuses on the elevated temperature behavior of the material pertaining to the heat-affected zone.

Nil Strength Temperature

For the present investigation, the peak temperature, for the Gleeble thermal cycle, was chosen as the nil strength temperature (NST). The NST of the alloy is the temperature at which the material loses all strength and ductility. NST was determined by placing a small constant load of 10 lb (4.5 kg) on the specimen and heating at the predetermined heating rate (corresponding to measured HAZ thermal cycle) until the specimen fractured. The temperature at which the

specimen fractured was taken as NST.

The average values of NST for Alloy 2091 in the as-cast and T3 condition are 550°C and 600°C (1022° and 1112°F), respectively. The eutectic temperature for the aluminum-lithium alloy is reported to be close to 520°C (968°F) (Ref. 13). Differential thermal analysis of Alloy 2091-T3 indicates the solidus temperature to be approximately equal to 540°C (1004°F). The experimentally observed NST for Alloy 2091 is well above these temperatures and may have been associated with some partial melting at the temperature. The NST for Alloy 2024 is close to 550°C.

Elevated Temperature Strength

The elevated temperature strength of the two heats of aluminum-lithium Alloy 2091 and Alloy 2024 was determined during heating to the peak temperature (on heating) and during cooling from the peak temperature (on cooling). First, the relative elevated temperature strength of the three heats "on heating" are presented in Fig. 3. The results show that, for the range of temperatures investigated, the ultimate tensile strength of Alloy 2091 compared very well with Alloy 2024. This is particularly significant since Alloy 2091 is developed for possible replacement of Alloy 2024 in structural applications. In the T3 condition, the room temperature strength of Alloy 2091 is approximately 425 MPa (61.6 ksi) and that of Alloy 2024 is approximately 475 MPa (68.9 ksi). The room temperature strength has been measured previously for the Soviet-developed 01420 (Al-5Mg-2Li-0.1Zr) alloys (Ref. 14) and 8090 (Al-2.5Li-1.2Cu-0.7Mg-0.12Zr) alloys (Ref. 15). These studies reported room temperature strength in the range of 400–425 MPa.

The elevated temperature mechanical properties have been measured for Al-Li-Mg (Refs. 11, 16) and Al-Li-Co (Ref. 17) alloys. These studies indicate that the elevated temperature strength of these alloys decrease rapidly, at temperatures exceeding 100°C (212°F), when these alloys contained zirconium. This rapid reduction in strength is attributed to dynamic recovery caused by the movement of dislocations to sub-boundaries in the alloy (Ref. 16). The results shown in Fig. 3 show that the 2091 alloy retains its high strength until about 200°C (392°F). Beyond this temperature, the strength decreases rapidly to a minimum measured value of 33 MPa (4.8 ksi) at 550°C. The improved performance of the 2091 alloy is apparently due to the presence of the T1 (Al_2CuLi) and the S′ (Al_2CuMg) phases at the subgrain boundaries and therefore, delaying the dynamic recovery. The elevated temperature strength of Alloy 2091 in the as-cast condition was relatively lower throughout the temperature regime. It is probably due to the large grain size of the cast material. Figure 4 is a typical photomicrograph of the base metal structure for the alloy in the as-cast condition, indicating a very coarse dendritic microstructure. The dark areas in the microstructure indicate the lithium rich δ (AlLi) phase.

During welding, the weld HAZ experiences temperatures far in excess of the transformation temperature (approximately 350°C) of the material. Therefore, an understanding of the mechanical behavior of the material in this temperature regime is particularly important to understand the HAZ crack sensitivity of the material (Ref. 18). A thermal cycle, with the experimentally determined heating and cooling rate and a peak temperature equaling the NST, was imposed on the gauge section of the Gleeble specimen. Elevated temperature mechanical properties were determined at the test temperature for all three heats during the

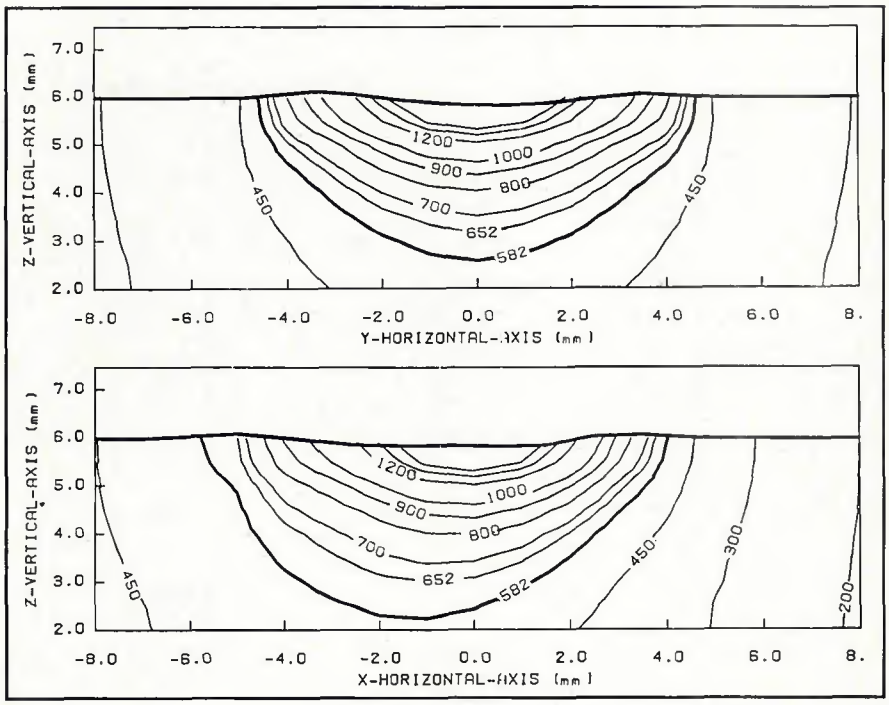

Fig. 2 — Typical temperature distribution in the longitudinal and transverse section of an autogenous GTA weld

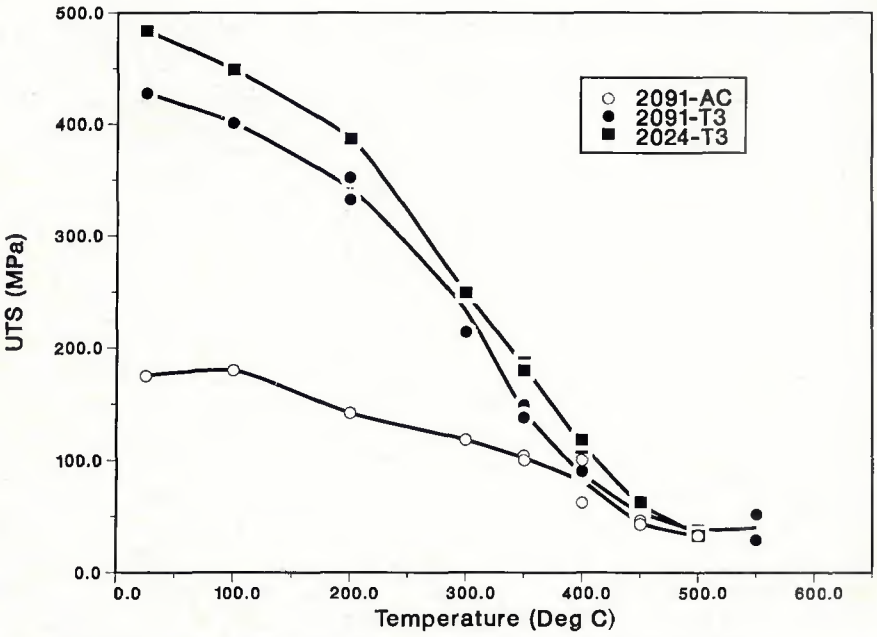

Fig. 3 — On-heating hot tensile test results for Alloys 2091-AC, 2091-T3 and 2024-T3

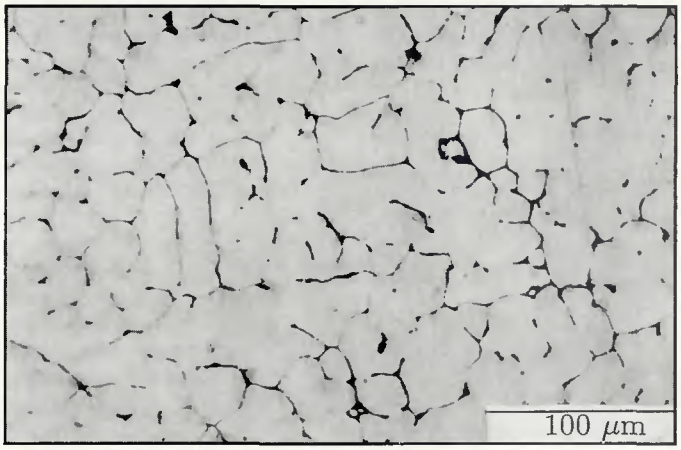

Fig. 4 – Typical photomicrograph of the as-cast structure of Alloy 2091

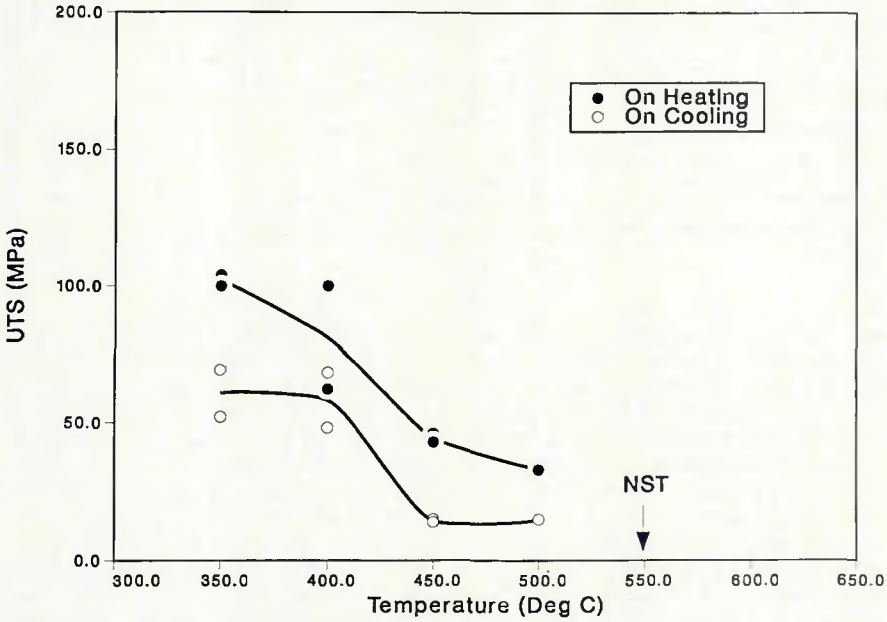

Fig. 5 – Hot tensile test results for Alloy 2091-AC

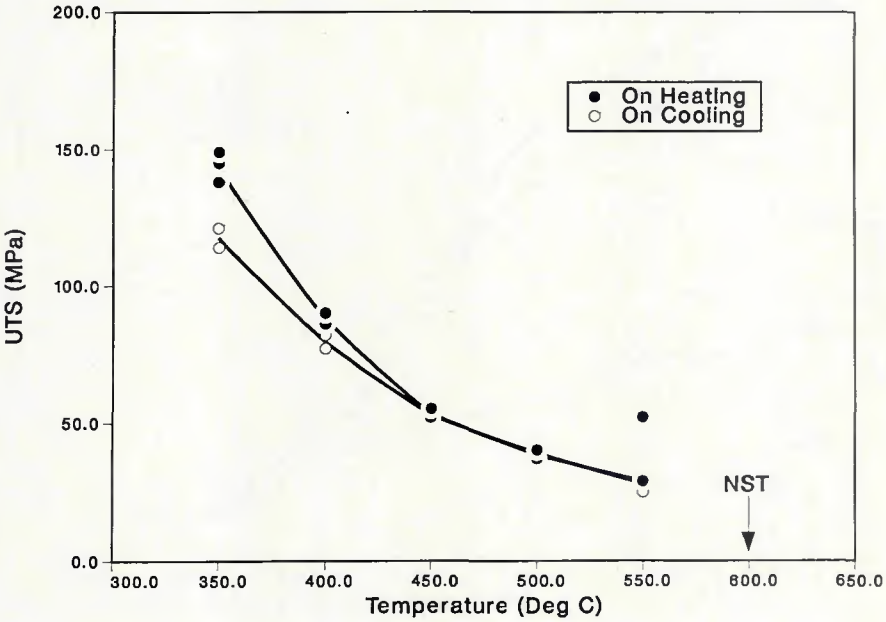

Fig. 6 – Hot tensile test results for Alloy 2091-T3

heat up (on heating) and the cool down (on cooling) phase of the thermal cycle. This was done to obtain a complete history of the variation in strength of weld HAZ during welding.

Figures 5–7 show the influence of the test temperature on the elevated temperature strength of the three heats. In general, for all three heats, the elevated temperature strength measured on cooling, as expected, was lower than the strength on heating. Alloy 2091 in the as-cast condition exhibited relatively poor strength for all the test conditions – Fig. 5. During the heating cycle, the tensile strength dropped rapidly from 100 MPa (14.5 ksi) at 350°C (662°F) to approximately 35 MPa (5.1 ksi) at 500°C (932°F). The results show that during the cooling cycle the material recovered only about 50% of the on-heating tensile strength.

The elevated temperature strength of the wrought Alloy 2091 in the T3 condition is shown in Fig. 6. During the on-heating cycle, the strength drops rapidly from 150 MPa (21.8 ksi) to about 30 MPa (4.4 ksi) at 550°C. Barring some scatter in the data, the results show that between 450°C (842°F) and the NST, the elevated temperature strength measured on heating and cooling did not differ significantly. For the test conditions considered in the present investigation, the maximum difference in strength of about 20 MPa (2.9 ksi) was observed at 350°C.

The result of the elevated temperature strength of wrought Alloy 2024-T3 is shown in Fig. 7. In general, Alloy 2024-T3 had relatively higher strength for all the test conditions. However, the results show that the elevated temperature strength measured on cooling is considerably lower than the strength measured on heating. The maximum difference in strength between the on-heating and the on-cooling test was close to 125 MPa (18.1 ksi) at 350°C. This is significantly larger than the difference in strength for Alloy 2091-T3, suggesting that the weld HAZ of Alloy 2024 may be more susceptible to hot cracks.

Hot Ductility

The hot ductility of the three heats considered in the present investigation was evaluated by measuring the reduction in area for the different testing conditions. The cross-sections at the fracture location for several of the specimens were elliptical due to anisotropy inherent in the material. Hence, the minimum and the maximum diameter at the fracture location were measured to determine the reduction in area.

Figure 8 shows the hot ductility response of Alloy 2091 in the as-cast condition. The maximum ductility of about 70% was observed at 450°C for the on-heating test. With further increase

in temperature, the ductility decreased rapidly to about 40% at 500°C. This is probably associated with the melting of the low melting (δ) constituent along the grain boundary. Optical metallography indicated partial melting of the alloy at elevated temperatures near the NST. The Gleeble hot ductility test depends on producing an isothermal plane, within the gauge length, perpendicular to the loading axis. The heat transfer from the gauge section is predominantly along the axis. Figure 9 is a photomicrograph of the longitudinal section of the fractured specimen tested close to the NST. The region in the center, indicated by the arrow, shows small dendrites along this axis where melting and subsequent solidification occurred at the grain boundary triple point. Fracture typically occurred intergranularly due to liquation and failure of the grain boundary constituent.

The on-cooling hot ductility results for Alloy 2091-AC show no recovery of ductility. For all the test conditions, Alloy 2091-AC shows zero ductility during the cooling phase of the thermal cycle. Figure 10 is the photograph of a typical specimen at the fracture location, indicating a brittle intercrystalline fracture. Examination of the surface indicates considerable oxidation and a very porous surface texture. The complete loss of ductility, as the material is cooled from the NST, is probably due to the deterioration in the surface of the specimen. Figure 11 is the longitudinal section, near the surface, of the specimen shown in Fig. 10. The microstructure shows the surface degradation due to oxidation and depletion of the lithium-rich (δ) phase.

Figure 12 shows the hot ductility response of the wrought Alloy 2091 in the T3 condition. The room temperature ductility of the alloy, as expected, was low (about 10%). This is attributed to the coherent δ′ (Al_3Li) precipitates, which impede the movement of dislocations. The ductility increased with increasing temperature to a maximum value of 96% at 450°C. The ductility did not decrease from this maximum value with further increase in test temperatures beyond 450°C.

Unlike the as-cast material, the wrought alloy exhibited a recovery of 70% ductility at 550°C. The lower ductility in comparison to the on-heating test at this temperature is probably due to liquated grain boundary (δ) constituent. The ductility further increased with decreasing temperature to a maximum of 95% at 400°C. Figure 13 is a photograph of the fracture surface indicating the tendency of the material to delaminate at elevated temperature. This is particularly evident from Fig. 14. The specimen in this case was subjected to a compressive stress resulting in delamination and fracture. Delamination typically occurs as a

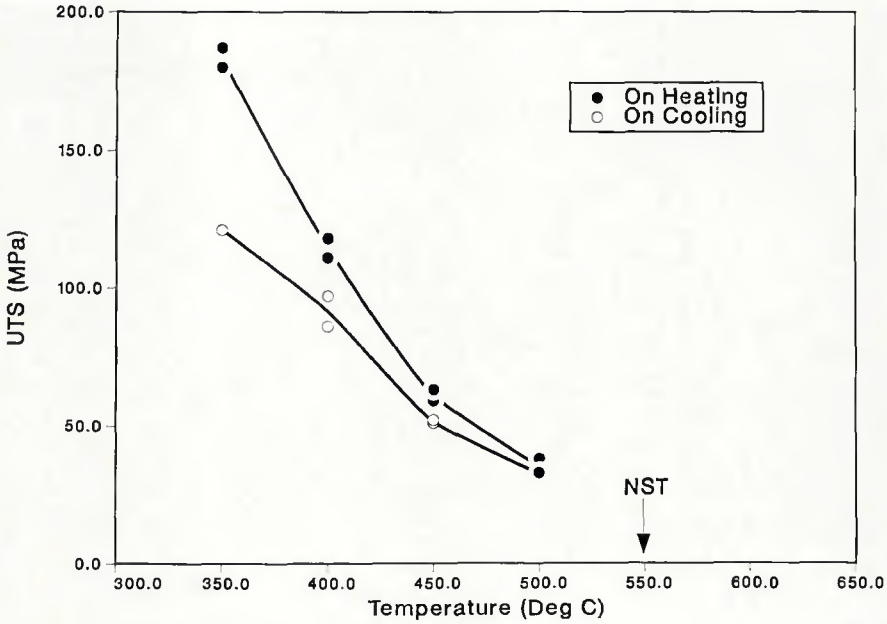

Fig. 7—Hot tensile test results for Alloy 2024-T3

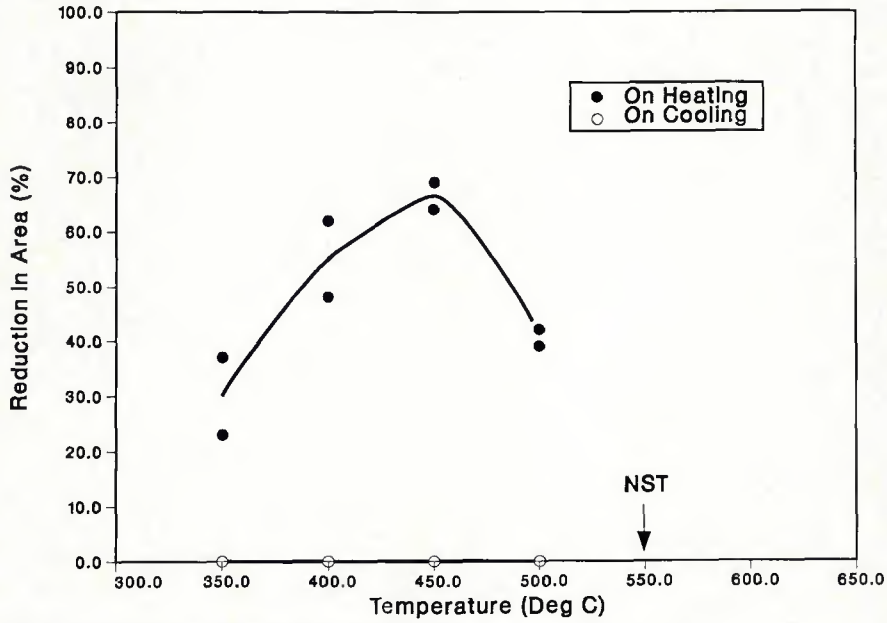

Fig. 8—Hot ductility test results for Alloy 2091-AC

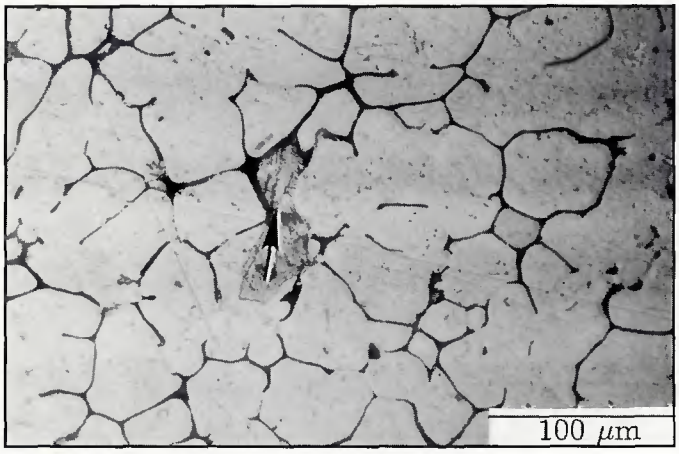

Fig. 9—Photomicrograph of the longitudinal section of the fractured specimen (Alloy 2091-AC, tested "on cooling" at 500°C)

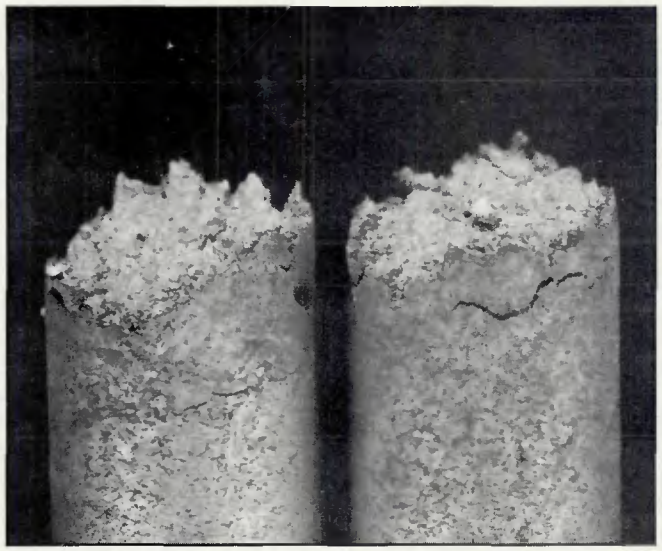

Fig. 10—Typical photograph of the fracture surface for Alloy 2091-AC (tested on cooling)

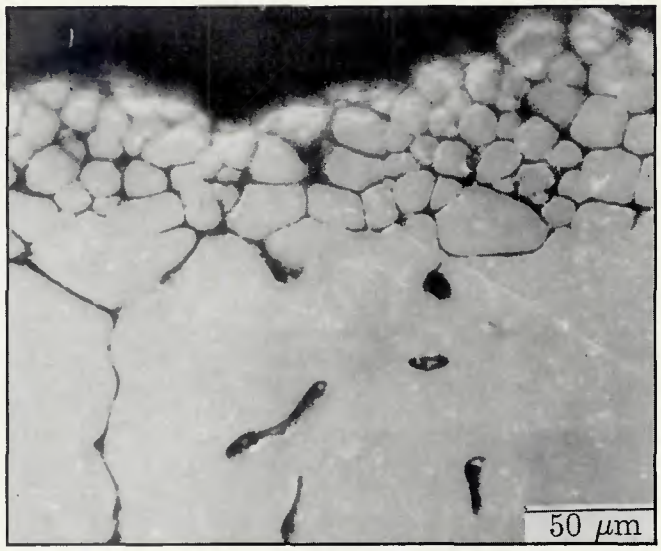

Fig. 11—Photomicrograph of the longitudinal section, near the surface, of the specimen shown in Fig. 10.

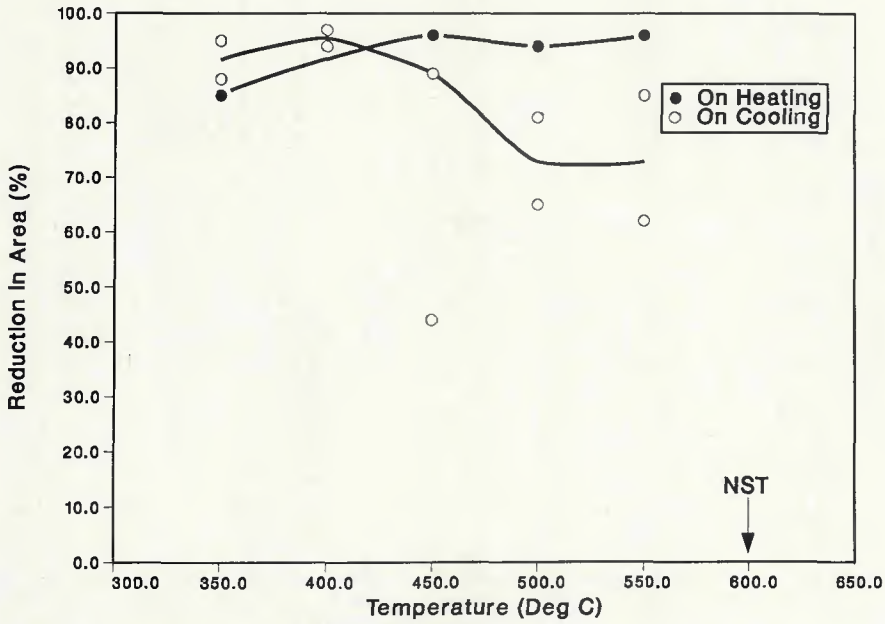

Fig. 12—Hot ductility test results for Alloy 2091-T3

Fig. 13—Typical photograph of the fracture surface for Alloy 2091-T3 (tested on cooling at 450°C)

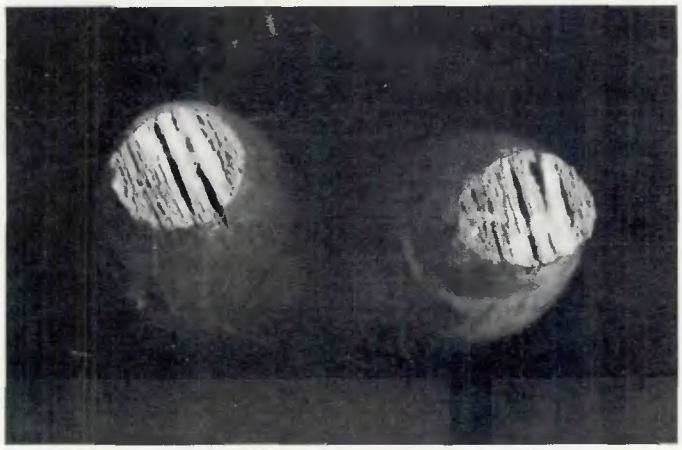

result of the rolling operation, which causes an elongated "pancake" structure in the rolling direction. At elevated temperatures, the low-melting phase forms a continuous liquid film parallel to the rolling direction, causing the material to delaminate.

Scanning electron microscopy (Fig. 15) of the test specimen at 450°C for the on-heating condition indicates coarse precipitates in the matrix and at the grain boundaries. Further increase in temperature resulted in the dissolution of these precipitates. This was particularly evident for the on-cooling tests where the specimens were heated to the NST and subsequently cooled to the test temperatures. Figure 16 is a micrograph of the longitudinal section, near the fracture, of the specimen tested at 550°C on cooling, indicating grain boundary decohesion. The matrix is devoid of any strengthening precipitates at this temperature. Upon further cooling, the solubility limit for the solute in the matrix decreases, resulting in precipitation. Typically, the δ' phase starts precipitating around 350°C. Figure 17 shows the SEM photomicrograph for the specimen at 350°C for the on-cooling test condition. The micrograph shows the slight decrease in ductility at this temperature is associated with the precipitation of fine second-phase particles, both within the matrix and along the grain boundaries.

The hot ductility results of Alloy 2024 T3 are shown in Fig. 18. The results show that with increasing temperatures the ductility of the material continued to increase to a maximum of 85% at 450°C and then decreased with further increase in temperature. Upon cooling, the material recovered ductility with decreasing temperature to a maximum measured value of 86%. However, the recovery of

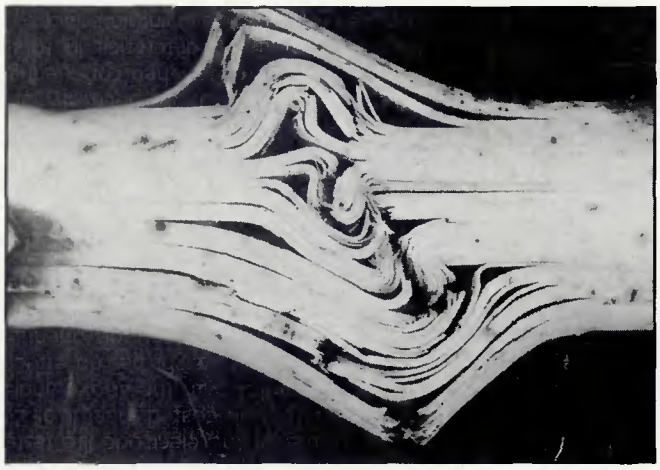

Fig. 14 — Photograph of Gleeble sample tested in compression indicating the tendency of wrought Alloy 2091 to delaminate

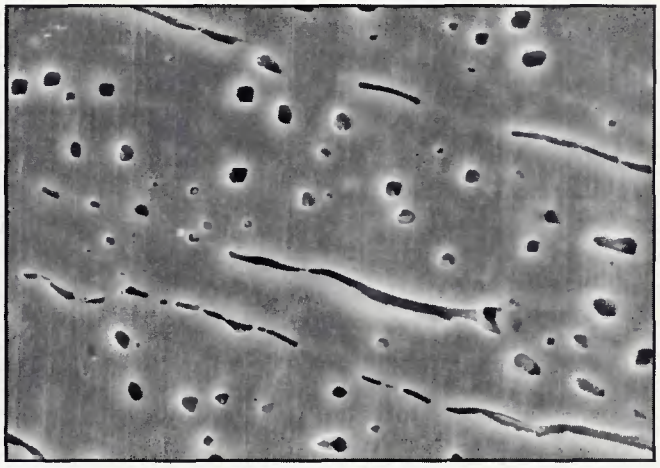

Fig. 15 — Photomicrograph of the longitudinal section of the fractured specimen (Alloy 2091-T3, test done on heating at 450°C)

Fig. 16 — Photomicrograph of the longitudinal section of the fractured specimen (Alloy 2091-T3, test done on cooling at 550°C)

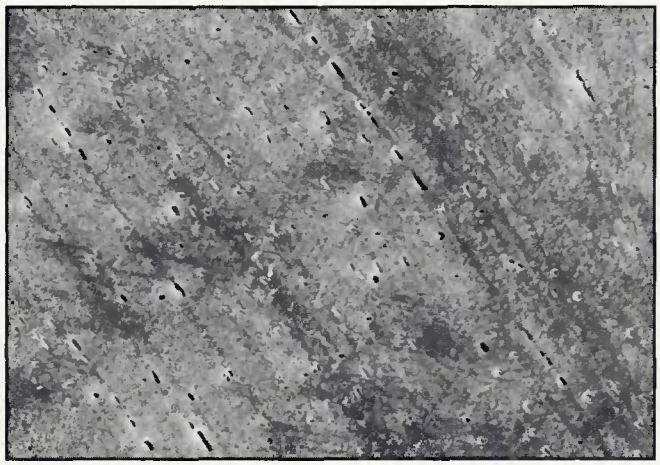

Fig. 17 — Photomicrograph of the longitudinal section of the fractured specimen (Alloy 2091-T3, test done on cooling at 350°C)

ductility was not as rapid as that exhibited by Alloy 2091 in the T3 condition. Fifty degrees below the nil strength temperature, Alloy 2024 exhibited a ductility of 15% in comparison to 75% for Alloy 2091.

SEM secondary electron image of the longitudinal section of the fractured specimen shows a coarsening of the grain boundary constituent with increasing test temperatures up to 450°C — Figs. 19 and 20. Further increase in test temperatures results in the dissolution of the precipitate in the bulk — Fig. 21. However, there were isolated pockets of large fragmented second-phase constituent. The low ductility exhibited by Alloy 2024 at 500°C on cooling is probably due to the liquation of these isolated pockets at the higher temperatures.

The strength-to-ductility ratio of Alloy 2024-T3, at the highest temperatures, is considerably larger than that for Alloy 2091-T3. This together with the significantly lower ductility of the Alloy 2024-

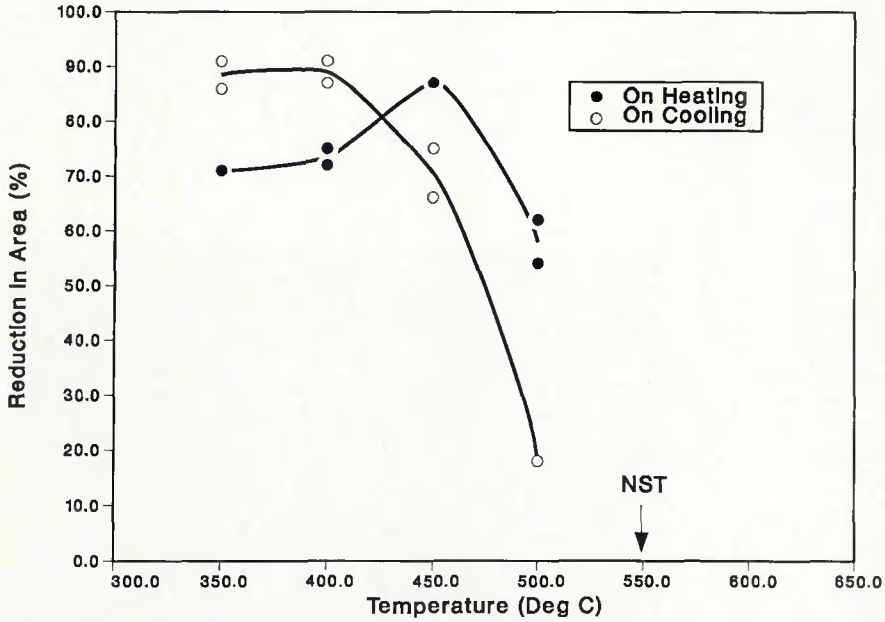

Fig. 18 — Hot ductility test results for Alloy 2024-T3

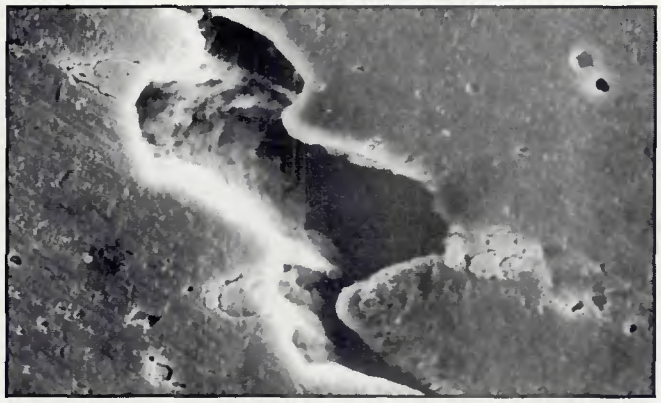

Fig. 19—Photomicrograph of the longitudinal section of the fractured specimen (Alloy 2024-T3, test done on heating at 350°C)

Fig. 20—Photomicrograph of the longitudinal section of the fractured specimen (Alloy 2024-T3, test done on heating at 450°C)

T3 at these temperatures indicates that Alloy 2024 is more susceptible to HAZ cracking. Alloy 2091-T3, on the other hand, is very ductile at temperatures close to the solidus temperature, suggesting that the material is resistant to hot-cracking in the weld metal HAZ.

Conclusions

A detailed experimental study was carried out to characterize elevated temperature mechanical properties of aluminum-lithium Alloy 2091. Results and conclusions are summarized as follows:

1) In general, Alloy 2091 in the as-cast condition exhibited very low elevated temperature strength and ductility. The relatively poor strength and ductility is apparently due to the coarse dendritic structure of the material.

2) The hot tensile tests indicated that tensile strength of wrought Alloy 2091 adequately matched the strength of Alloy 2024 throughout the temperature regime. This is particularly encouraging since Alloy 2091 was developed for replacing Alloy 2024 in aerospace applications.

3) The elevated temperature strength measured for Alloy 2024 "on cooling" was considerably lower than the strength measured "on heating". The maximum difference in strength between the on-heating and on-cooling test for Alloy 2024 was 125 MPa at 350°C in contrast to 20 MPa for Alloy 2091 at the same temperature.

4) The results of hot ductility test show that Alloy 2091 in the wrought form exhibits superior ductility throughout the range of temperatures investigated. In particular, 50°C below the NST, Alloy 2091-T3 exhibits excellent recovery of ductility (70%) in comparison to Alloy 2024-T3 (15%). This would indicate lower weld metal HAZ crack susceptibility for Alloy 2091.

Acknowledgment

The authors would like to thank Mr. R. P. Martukanitz of Alcoa Technical Center, for the material and technical support provided during this investigation.

Fig 21—Photomicrograph of the longitudinal section of the fractured specimen (Alloy 2024-T3, test done on heating at 550°C)

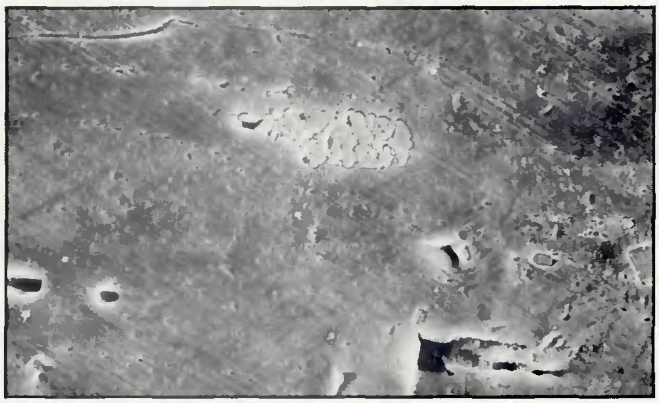

References

1. Wald, G. G. 1981. NASA Contractor report 16576, NASA, Washington, D. C.

2. Sankaran, K. K., and Grant, N. J. 1980. *Proceedings of the 1st International Aluminum-Lithium Conference.* Stone Mountain, Ga. Edited by T. H. Sanders, Jr. and E. A. Starke, Jr., TMS-AIME, Warrendale, Pa., 1981, p. 206.

3. Quist, W. E., Narayanan, G. H., and Wingert, A. L. 1983. *Proceedings of the 2nd International Aluminum-Lithium Conference.* Monterey, Calif. Edited by E. A. Starke, Jr. and T. H. Sanders, Jr., TMS-AIME, Warrendale, Pa. 1984, p. 206.

4. Cieslak, S. J., Hart, R. M., Mehr, P. L., and Mueller, L. N. 1985. Presented at the 17th international SAMPE technical conference, October 22–24, Kiamesha Lake, N. Y.

5. Archbutt, S. L., Grogan, J. D., and Jenkin, J. W. 1928. *J. Inst. Metals* 40:219.

6. Singer, A. R. E., and Cottrell, S. A. 1946. *Jour. Inst. Met.* 72:33.

7. Pumphrey, W. I., and Jennings, P. H. 1948. *Jour. Inst. Met.* 75:235.

8. Nippes, E. F., Savage, W. F., Bastian, B. J., Mason, H. F., and Curran, R. M. 1955. *Welding Journal* 34:183-s.

9. Savage, W. F., and Krantz, B. 1966. *Welding Journal* 45:13-s.

10. Canonico, D. A., Savage, W. F., Werener, W. J., and Goodwin, G. M. 1969. WRC publication, July, p. 68.

11. Balaguer, J. P., Nippes, E. F., and Walsh, D. W. 1986. *Proceedings of an International Conference in Welding Research.* Gatlinburg, Tenn., p. 723.

12. Zacharia, T., Eraslan, A. H., and Aidun, D. K. 1988. *Welding Journal* 67:18-s.

13. Martukanitz, R. P. 1987. Aloca Technical Center, Pittsburgh, Pa.

14. Pickens, J. R., Langan, T. J., and Barta, E. 1986. *Proceedings of the Third International Aluminum-Lithium Conference.* University of Oxford, July 1985. Edited by C. Baker, P. J. Gregson, S. J. Harris, and C. J. Peel, The Institute of Metals, London, England, p. 137.

15. Pridham, M., Noble, B., and Harris, S. J. 1984. *Proceedings of the 2nd International Aluminum-Lithium Conference.* Monterey, Calif. Edited by E. A. Starke, Jr. and T. H. Sanders, Jr., TMS-AIME, Warrendale, Pa. 1984, p. 547.

16. Noble, B., Harlow, K., and Harris, S. J. 1984. *Proceedings of the 2nd International Aluminum-Lithium Conference.* Monterey, Calif. Edited by E. A. Starke, Jr. and T. H. Sanders, Jr., TMS-AIME, Warrendale, Pa. 1984, p. 65.

17. Sastry, S. M. L., and O'Neal, J. E. 1984. *Proceedings of the 2nd International Aluminum-Lithium Conference.* Monterey, Calif. Edited by E. A. Starke, Jr., and T. H. Sanders, Jr., TMS-AIME, Warrendale, Pa. 1984, p. 79.

18. Aidun, D. K., Zacharia, T., and Martukanitz, R. P. Hot cracking susceptibility of Al-Li-Cu-Mg alloy. Fourth International Conference on Aluminum Weldments, INALCO '88, Tokyo, Japan, April 4–12, 1988.